Desalination and Water Treatment
www.deswater.com

doi:10.5004/dwt.2017.20226

66 (2017) 23–35
March

Thin-film composite forward osmosis membrane in rejecting trace organic compounds: Impact of molecular charge

Yan-Ling Liu[a], Fan-Xin Kong[a,b], Xiao-Mao Wang[a,*], Hong-Wei Yang[a], Yuefeng F. Xie[a,c]

[a]*State Key Joint Laboratory of Environment Simulation and Pollution Control, School of Environment, Tsinghua University, Beijing 100084, China, Tel. +86-10-6278 1386, email: wangxiaomao@tsinghua.edu.cn*
[b]*School of Chemical Engineering, China University of Petroleum, Beijing 102249, China*
[c]*Environmental Engineering Programs, The Pennsylvania State University, Middletown, PA, 17057, USA*

Received 19 June 2016; Accepted 12 September 2016

ABSTRACT

The performance of a thin-film composite (TFC-ES) polyamide forward osmosis (FO) membrane in rejecting pharmaceuticals (PhACs) was investigated and compared with two asymmetric cellulose triacetate (CTA-ES and CTA-NW) membranes. Results showed that the TFC-ES membrane had a higher water permeability and salt rejection ability, but a poorer performance in rejecting the selected 21 PhACs (as a sum) than both CTA membranes. The TFC-ES membrane exhibited a better rejection of the negatively charged PhACs than the positively charged and neutral PhACs as theoretically predicted based on membrane surface charge. That the permeability coefficient values for all the positively charged PhACs determined in the FO mode were larger than that in the reverse osmosis mode was speculated to result from the impact of reverse draw solute diffusion on FO rejection of those PhACs. "Ion exchange" might be the mechanism, which could make additional contribution to the transport of positively charged PhACs and result in lower rejections than as expected. In addition to steric exclusion and electrostatic effect, the PhAC–membrane interactions could also play an important role in the transport of PhACs and affect the rejection by the FO membranes.

Keywords: Forward osmosis (FO); Permeability coefficient; Ion exchange mechanism; Thin-film composite (TFC) membrane; Trace organic compounds (TrOCs)

1. Introduction

Forward osmosis (FO) is a promising technology for wastewater reclamation. The technology is particularly attracting when low-cost energy is available that can be utilized for the extraction of reclaimed water and re-concentration of the diluted draw solution [1–3]. The FO operation on its own features a negligible energy consumption, a high water recovery, and a low fouling propensity [4,5]. However, one of the biggest hindrances to the practical applications of FO technology to wastewater reclamation was the relatively low performance in water permeation and salt rejection. A low water permeability demands a large membrane area, and a poor salt rejection leads to a fast loss of draw solute. Most of the first-generation FO membranes were made of cellulose triacetate (CTA) material. The thin-film composite (TFC) FO membranes were later introduced, which have demonstrated improved water productivity and salt rejection [6–8]. It appears that the TFC FO membranes have a higher promise in wastewater reclamation. Nevertheless, the TFC FO membranes must outperform or, for the least, be comparable to the CTA membranes in rejecting trace organic compounds (TrOCs). TrOCs are ubiquitously present in the secondary effluent and pose potential hazards to the ecosystem and human health if not sufficiently removed [9].

It was well documented that the CTA FO membranes could have an ability comparable to reverse osmosis (RO) membranes in rejecting the various TrOCs [10–13], and the more compact NW-type membrane performed somewhat

*Corresponding author.

better than the less compact ES-type membrane. (The ES type membrane has an embedded polyester screen mesh while the NW type has a non-woven backing consisting of polyester fibers.) Studies on TrOC rejection by TFC FO membranes are relatively scarce. A TFC membrane is different from a CTA membrane in a number of membrane properties. It was speculated that the TFC membrane might have a smaller effective "pore" size partly due to the existence of a thicker hydration layer inside the pores. The TFC membranes are normally more negatively charged than the CTA membranes at neutral pH [14]. Moreover, TFC membranes were believed to be less hydrophobic than CTA membranes [15]. According to the hindered transport theory, the rejection of a contaminant by a dense membrane is determined by a combination of the steric effect, electrostatic effects and hydrophobic interactions [16–18]. As such, the distinctions in molecular-weight-cut-off (MWCO), surface charge and hydrophobicity would lead to the difference in TrOC rejection by the TFC and CTA membranes.

Among the few experimental studies, Jin et al. [19] found that while the lab-made TFC and commercial ES-type CTA membranes performed similarly well in rejecting the neutral carbamazepine and the negatively charged diclofenac at circum-neutral pH, the TFC membrane performed better in rejecting the negatively charged ibuprofen and naproxen. A later study by Xie et al. [14] compared the performance of a commercial TFC membrane and an ES-type CTA membrane. They found that the rejection of some neutral TrOCs by the TFC membrane was substantially higher, but the rejections of the positively charged amitripltyline and trimethoprim and the negatively charged sulfamethoxazole, diclofenac and bezafibrate were comparable. Recently, Zheng et al. [20] found that the rejection of the negatively charged tetracycline by a commercial TFC membrane was lower than both the ES- and NW-type CTA membranes. Generally, the previous studies did not unambiguously show the better rejection of negatively charged TrOCs than the neutral and positively charged TrOCs by TFC membranes, which was otherwise predicted by theoretical analysis. Further study is required in which more TrOCs, positively charged in particular, need to be included.

Reverse draw solute diffusion is a characteristic feature of FO operation, which was shown to impact the rejection of some TrOCs in a few previous studies. Xie et al. [21] first observed this phenomenon and proposed that the draw solute diffusion retarded the mass transport of some hydrophobic TrOCs and therefore enhanced the rejection. We later found that the rejection of several negatively charged TrOCs of small molecular weight in FO mode was lower than that in RO mode [22]. It was speculated that ion exchange might occur between the TrOCs and the reversely diffused draw solute within the membrane. Nevertheless, whether reverse draw solute diffusion affects rejection of TrOCs by TFC membranes remains yet to be known.

In this study, a TFC FO membrane was tested for its performance in rejecting a total of 21 pharmaceuticals (PhACs), which were selected to have different molecular charge and hydrophobicity. The rejection was compared with that by ES- and NW-type CTA membranes we reported recently [22]. Efforts were made to elucidate the impacts of electrostatic effects and hydrophobic interactions as well as reverse draw solute diffusion on rejection of TrOCs during FO operation using the TFC membrane.

2. Materials and methods

2.1. The FO membrane and setup

The TFC FO membrane (TFC-ES) was obtained from Hydration Technologies, Inc. (Albany, OR). The membrane had a polyamide active layer casted on an embedded polyester screen mesh. According to the specifications, the membrane was rinsed by immersing first in a 25% isopropanol (Fisher Scientific, USA) solution for 30 min and then in an ultrapure water (Milli-Q, Millipore) for at least 12 h at room temperature prior to use.

A bench-scale cross-flow FO setup was employed to investigate the performance of the TFC FO membrane in rejecting a sum of 21 selected PhACs. The system had been used to test the performance of two CTA FO membranes (i.e., CTA-ES and CTA-NW) in our previous study [22]. The system consisted of a lab-made FO cell which was used to hold an FO membrane coupon to separate the feed water and the draw solution flow channels, a feed water tank and a draw solution tank, two variable-speed gear pumps (Longer, USA) for feed water and draw solution recirculation, a digital balance (Mettler Toledo, Germany) for measuring the FW weight change, and a computer for data logging. The effective membrane area was 40.5 cm^2, and the flow channel heights were both 2 mm. No mesh spacers were used.

For a more convenient comparison, the operating conditions were identical to those adopted to test the CTA membranes [22]. In more details, the FO experiments were conducted in an air-conditioned room at 25 ± 1°C. The flow directions of the FW and the DS were counter-current with flow velocities both at 21.4 cm/s. The FW was a combined solution of 21 PhACs (Sigma-Aldrich, Germany) each having a concentration at 100 μg/L. The FW also contained 10 mM NaCl as background electrolytes and 0.1 mM $NaHCO_3$ for pH buffering (at 7.0 ± 0.2). Some of the key physicochemical properties of the PhACs are presented in Table 1. At neutral pH, eight, eight and five PhACs are positively charged, negatively charged and neutral, respectively. A series of NaCl solutions of increasing concentration (0.1, 0.5, 1, 2, and 3 M) were used as the DS to generate increasing osmotic pressure difference and water flux. (The FO membrane was first rinsed for 2 h by using Milli-Q water as the FW and 0.1 M NaCl solution as the DS.) An equilibration period of 24 h was set for the adsorption of PhACs, if any, onto the membrane matrix when the first DS (0.1 M NaCl solution) was used. At each draw solution concentration condition, the FO system was continuously run for at least 6 h before the determination of water flux and sampling of both FW and DS for PhAC concentration determination. Because the DS would be continuously diluted during the FO operation, a concentrated NaCl solution (5 M) was added to the DS intermittently to maintain its concentration variation within 5%. The added volume was determined according to the water flux and time intervals on the premise that the loss of draw solute due to the reverse draw

Table 1
Physicochemical properties for the investigated PhACs.

	Charge (pH = 7)	MW (g/mol)	LogD (pH = 7)[a]	Stokes radius (nm) [b]
Nizatidine	Positive	331.5	–0.88	0.5
Diltiazem		414.5	2.98	0.57
Erythromycin		733.9	0.81	0.83
Sulpiride		341.4	–1.44	0.48
Metoprolol		267.4	–0.81	0.47
Propranolol		259.3	1.15	0.46
Ranitidine		314.4	–1.44	0.5
Roxithromycin		837	1.75	0.9
Carbamazepine	Neutral	236.3	1.89	0.39
Cephalexin-hydrate		365.4	–2.68	0.47
Chloramphenicol		323.1	1.10	0.45
Ciprofloxacin		331.3	–0.33	0.47
Norfloxacin		319.3	–0.65	0.47
Diclofenac	Negative	296.1	1.77	0.45
Gemfibrozil		250.3	2.07	0.46
Indomethacin		357.8	1.29	0.5
Nalidixic acid		232.2	–1.20	0.46
Clofibric acid		214.6	–1.06	0.38
Sulfadiazine		250.3	–0.68	0.4
Sulfamethazine		278.3	0.15	0.42
Sulfamethoxazole		253.3	–0.22	0.39

[a]obtained from the SciFinder Scholar database; [b] calculated from the Stokes-Einstein equation.

solute diffusion was negligible. All samples were stored at –18°C and analyzed within two days.

The water flux (J_w) was determined by measuring the decrease of the FW volume (V_{FW}) as a function of time (t), i.e., $J_w = dV_{FW}/dt/A_m$, where A_m is the effective membrane area. The PhAC flux (J_{PhAC}) was calculated from the increase of PhAC concentration in the DS (c_{DS}) with time by $J_{PhAC} = d(V_{DS}c_{DS})/dt/A_m$, where V_{DS} is the DS volume which is the total volume of initial DS, permeate water and added 5 M NaCl solution. The rejection of a PhAC (R_{PhAC}) can be calculated from the water and PhAC fluxes by

$$R_{PhAC} = 1 - \frac{J_{PhAC}}{J_w c_{FW}} \tag{1}$$

where c_{FW} is the PhAC concentration in the FW.

2.2. Determination of permeability coefficients

Performance of an FO membrane, in terms of water productivity and rejection of the draw solute and each PhAC, is dictated by the permeability coefficients of water (A), draw solute (B_i) and the PhACs (B_{PhAC}), respectively. These permeability coefficients are intrinsic membrane properties, and are theoretically independent of the operating conditions such as draw solute concentration and cross-flow velocities.

According to the solution–diffusion model [23,24], the water flux (J_w) and rejection of a PhAC (R_{PhAC}) during FO operation can be described by

$$J_w = A\left(\pi_{DS}\exp\left(\frac{-J_w S}{D_{DS}}\right) - \pi_{FW}\exp\left(\frac{J_w}{k_i}\right)\right) \tag{2}$$

$$R_{PhAC} = \frac{J_w}{J_w + B_{PhAC}\exp\left(\frac{J_w}{k_{PhAC}}\right)} \tag{3}$$

where π_{DS} and π_{FW} are the osmotic pressures for the DS and FW, respectively, k_i and k_{PhAC} are the mass transfer coefficients for the FW background electrolyte and PhAC, respectively, accounting for the effect of concentrative external concentration polarization (ECP) on the FW side, D_{DS} is the draw solute diffusion coefficient and S is the membrane structure parameter. It should be noted that Eq. (2) did not include the effects of reverse draw solute flux and dilutive ECP on the DS side [25,26]. Calculation showed that the mass transfer coefficients (k_i and k_{PhAC}) were in order of 10^{-5} m/s, which were 1–2 orders of magnitude higher than the water flux. (Equations for the calculation of k could be found in Section 1 in the Supplemental File.) Therefore, the effect of concentrative ECP on the water flux and solute rejection could be neglected in the calculation, i.e., $\exp(J_w/k)\approx 1$. As such, the B_{PhAC} value of each PhAC can be deduced by fitting of the experimentally obtained rejections using Eq. (3). In this study, this method is denoted as the "fitting method".

If an FO membrane is operated in the RO mode, rejection of a PhAC can also be mathematically described by Eq. (3). This method of determining the B_{PhAC} values is denoted as the "RO-mode method". Moreover, the water flux and rejection of the containing inorganic salts could be described by

$$J_w = A\left(\Delta P - \Delta\pi\exp\left(\frac{J_w}{k_i}\right)\right) \tag{4}$$

$$R_i = \frac{J_w}{J_w + B_i\exp\left(\frac{J_w}{k_i}\right)} \tag{5}$$

where ΔP is the applied hydraulic pressure, $\Delta\pi$ is the osmotic pressure difference across the membrane, k_i is the mass transfer coefficient for the inorganic salt (during RO operation).

The cross-flow RO system used for the determination of the permeability coefficients in the RO mode was identical to that described in our previous study [22]. In brief, the system consisted of three parallel filtration cells (CF042P, Sterlitech, USA) holding the FO membranes, a feed tank of 36 L in volume thermostated at 25 ± 1°C, a high-pressure diaphragm pump (Hydro-Cell D10, Wanner Engineering, USA), a number of pressure and flow-rate sensors, and other accessories. The filtration cells were made of Teflon with an effective area of 42 cm^2 each. The feed tank, the tubing and the valves were all made of stainless steel. A relatively high cross-flow velocity at 30.4 cm/s was adopted

throughout the test. It was assumed that the cross-flow velocity was sufficiently high to alleviate the external concentration polarization and as such the exponential term $\exp(J_w/k_i)$ was approximately equal to 1. During the filtration, all permeates from filtration cells were returned to the feed tank, except when sampled for chemical analysis.

An ultrapure water (with an osmotic pressure of zero) was filtered to determine the A value according to Eq. (4). A 10 mM NaCl solution was filtered to determine the B_i value according to Eq. (5). A mixed TrOC solution which was identical to the feed water for FO experiments was filtered to determine the B_{PhAC} values in the RO mode. The glucose rejection of the FO membrane was also determined by filtering a 10 mg/L glucose solution. A fresh FO membrane was used for each filtration. A set of step-increased filtration pressures from 2 to 8 bar were adopted for each filtration. At each adopted pressure, after a stabilization period of 6–12 h, the water flux was determined and the feed and permeate water were sampled for NaCl or PhAC measurement.

2.3. Membrane characterization

The zeta potential of the membrane was measured in a background solution containing 10 mM KCl using a zeta potential analyzer (Delsa Nano, Beckman, USA). The PhAC-membrane interaction free energy (ΔG_i) was calculated from the surface free energy components of the PhAC and the membrane [27,28]. The surface free energy components of the FO membranes were determined by measuring contact angles using three different liquids (i.e., water, diiodomethane and formamide) on the membrane surface and solving the Young-Dupré equation [29,30]. (More details of the ΔG_i calculation could be found in Section 2 in the Supplemental File.) Contact angle was measured using a goniometer (Contact Angle System OCA20, Data Physics Instruments GmbH, Germany) following a standard sessile drop method. The membranes were rinsed and dried in a desiccator at room temperature for at least 24 h prior to the measurement. Since the FO membranes were not flat in the dry state, they were stuck on glass slides by double side tapes before conducting the contact angle measurement.

2.4. Analytical methods

The PhAC concentrations were determined by using an ultra-performance liquid chromatograph–tandem mass spectrometer (LC1290/QQQ6460, Agilent) in the electrospray ionization (ESI) multiple reaction monitoring mode. More details could be found in our previous study [22]. The NaCl concentration was deduced from the chloride ion concentration, which was detected by using ion chromatography (Metrohm, Switzerland). The concentration of glucose was determined by using the phenol–sulfuric acid method [31].

3. Results and discussion

3.1. Water permeation and salt rejection

The water permeation rate through the TFC-ES membrane at different draw solute (NaCl) concentrations was determined (Fig. 1) and compared with that through the CTA-ES and CTA-NW membranes [22]. It was clear that the TFC-ES membrane had a higher water productivity than both CTA membranes. At a typical draw solute concentration of 1.0 M, the water flux was 4.72×10^{-6}, 3.46×10^{-6} and 1.8×10^{-6} m/s, respectively. The higher water productivity of the TFC-ES membrane was partly due to the higher water permeability coefficient (A value) (Table 2). The water permeability was determined by operating the FO membrane in RO mode. The determined water permeability for the TFC-ES membrane (3.86×10^{-7} m/s/bar) was 1.6- and 2.7-fold of that for the CTA-ES and CTA-NW membranes, respectively.

The higher water productivity was also partly due to the smaller membrane structural parameter (S value). The membrane structural parameter is an intrinsic physical property of an FO membrane [32,33]. A lower value for membrane structural parameter is preferred because it reduces the extent of internal concentration polarization. The membrane structural parameter values were determined by fitting the experimental data (Fig. 1) using Eq. (2). They were 496, 480 and 700 μm for the TFC-ES, CTA-ES and CTA-NW membranes, respectively. It should be noted that the S values were determined by an indirect method and the errors of other parameters could lead to the inaccurate calculation.

The salt (NaCl) permeability coefficient (B_i value) was also determined for the membrane (Table 2). It was revealed that the TFC-ES membrane had a salt permeability coefficient in between the two CTA membranes. The perm-selectivity (B_i/A) of the membrane was calculated. It can be found that the salt separation ability of the TFC-ES membrane was better than the CTA-NW membrane, and better than the CTA-ES membrane even more. In addition, given the perm-selectivity of a membrane, the reverse draw solute (NaCl) flux (J_{DS}) in FO operation could be predicted by $(J_{DS}/J_w) = (B_i/AnRT)$, where n is the number of dissolved species of the draw solute (2 for NaCl), R is the universal gas constant and T is the absolute temperature [24]. The reverse draw solute fluxes for the three FO membranes were calculated (Section 3

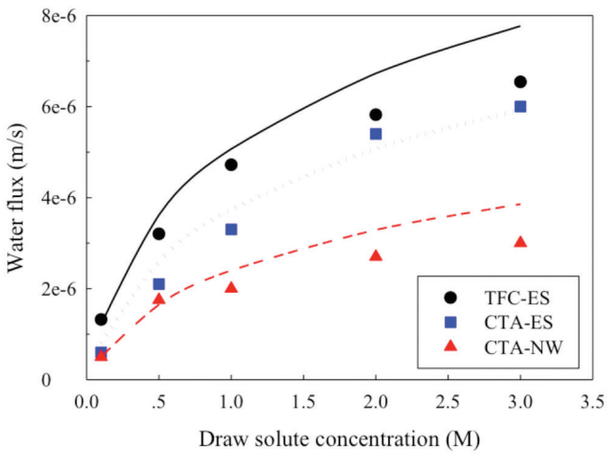

Fig. 1. The experimentally-obtained (dots) and model-fitted (lines) water fluxes of the three membranes as a function of draw solute concentration.

Table 2
Transport parameters of the FO membranes

Membrane	TFC-ES	CTA-ES	CTA-NW	TFC[a]	TCK-N[b]	TFC-1[c]	TFC-2[c]
Source	HTI	HTI	HTI	Oasys Water	Toray Chemical Korea	Lab-made	Lab-made
Pure water permeability, A ($\times 10^{-7}$ m/s/bar)	3.86	2.39	1.42	13.05	18.3	3.4	5.1
Salt(NaCl) permeability, B_i ($\times 10^{-7}$ m/s)	1.72	2.89	0.92	0.44	3.31	0.49	0.94
Perm-selectivity, B_i/A (bar)	0.45	1.21	0.65	0.03	0.18	0.14	0.18
Membrane structural parameter, S (μm)	496	480	700	520	460	—	—

[a]data from Ref. [14]; [b]data from Ref. [37]; [c]data from Ref. [19].

in the Supplemental File) and it was shown that at the same draw solute concentration, the TFC-ES membrane had the minimum reverse draw solute flux compared to the two CTA membranes. One advantage of fabricating TFC FO membranes is the independent optimization of the support layer and the polyamide active layer, thus improving the overall membrane performance [34]. Generally, the determined water and salt permeability coefficients, the perm-selectivity and the structural parameter of the TFC-ES membrane were similar to that reported in the literature [35,36]. Compared to other commercialized or lab-made TFC membranes [14,19,37], the TFC-ES membrane from HTI has a medium water productivity and structure parameter, but a relatively poorer salt separation ability (Table 2). However, care should be taken in that there might be some discrepancies between the transport parameters of FO membranes determined by the "RO + FO method" (i.e., RO experiments to determine A and B_i, and a following FO experiment to calculate S) and the true membranes properties exhibited in the FO mode, which could be mainly attributed to the difference of driving forces in the RO and FO processes [38,39]. It might be the reason for the slight deviation of the predicted water flux from the experimental-obtained water flux (Fig. 1).

3.2. Rejection of trace organic compounds

The performance of the TFC-ES membrane in rejecting the 21 PhACs were determined at different draw solute concentrations (Fig. 2). Generally, rejection of each PhAC was higher at a higher draw solute concentration (and water flux). When the draw solute concentration was sufficiently high (e.g., 2 M), all PhACs could be well rejected with a rejection higher than 85%. Nevertheless, as theoretically predicted, the TFC-ES membrane had a better rejection of the negatively charged PhACs than the positively charged PhACs (Fig. 3). As long as the draw solute concentration was higher than 1 M, the rejection of all negatively charged PhACs was higher than 90%. It also appeared that a negatively charged PhAC of a higher molecular weight could be more highly rejected by the TFC-ES membrane. In comparison, rejection of almost all positively charged PhACs was lower than 90% when the draw solute concentration was 1 M. Especially notable are erythromycin and roxithromycin, which both have a molecular weight higher than 700 Da but were not highly rejected

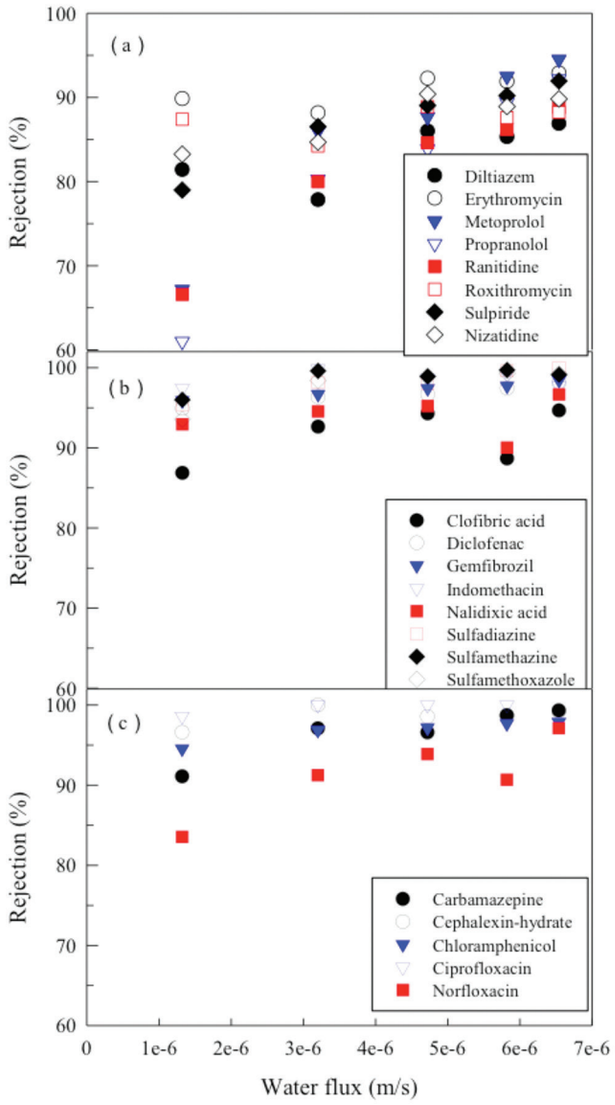

Fig. 2. The rejection of (a) positively charged PhACs (b) negatively charged PhACs and (c) neutral PhACs by the TFC-ES membrane in the FO mode.

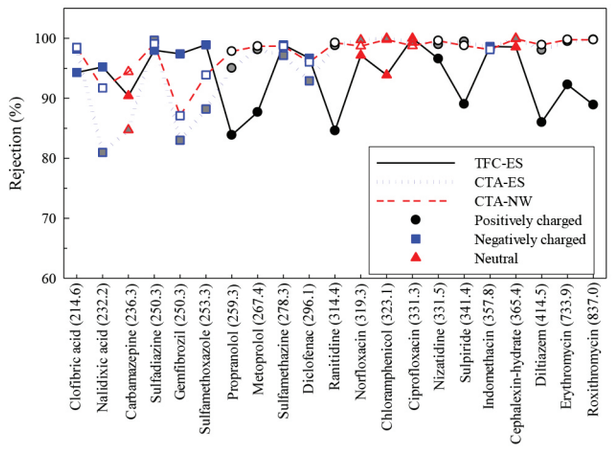

Fig. 3. Rejection of the 21 individual PhACs by the three membranes at the draw solute concentration of 1 M. The molecular weight (in Da) is shown in the parentheses.

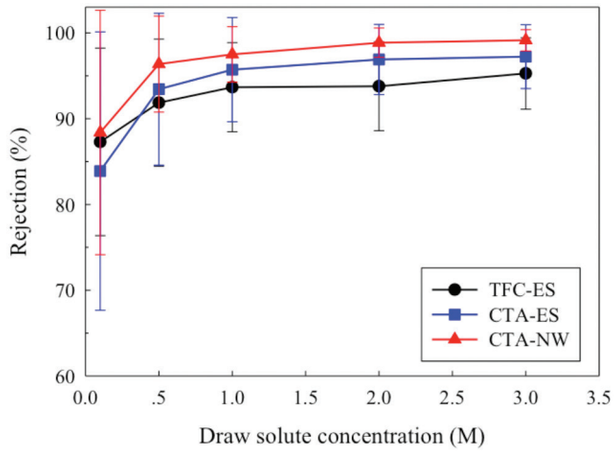

Fig. 4. The mean rejection of the 21 PhACs by the three membranes as a function of draw solute concentration.

by the TFC-ES membrane. Generally, rejection of uncharged PhACs was in between the negatively charged and positively charged PhACs.

Rejection of some of the selected PhACs (e.g., carbamazepine, diclofenac, sulfamethoxazole) was also investigated in previous studies [14,19]. The determined rejection complied well with that reported in those studies. However, the discrimination of rejection in terms of molecular charge was not intentionally investigated previously. Even though, Huang et al. [40] demonstrated that the positively charged metoprolol was much less rejected (at 82%) than the negatively charged sulfamethoxazole (at 95%) and the uncharged triclosan (at 97%) by the TFC-ES membrane. Including more TrOCs, Blandin et al. [41] reported that the TFC membranes allowed for very high rejection of negatively charged compounds but lower rejection of positively charged molecules, as a consequence of electrostatic interactions.

Since the TFC-ES membrane had a slightly higher rejection for the negatively charged PhACs while a substantially lower rejection for the positively charged PhACs compared to the CTA membranes, the TFC-ES membrane exhibited a poorer performance in rejecting the 21 selected PhACs (as a sum) than not only the more dense CTA-NW membrane but also the less dense CTA-ES membrane, especially when the draw solute concentration was sufficiently high (Fig. 4). This result was somewhat contradictory to those reported previously that the TFC membrane had a better performance than the CTA membranes in rejecting TrOCs [14,19]. It was probably due to the limited number of positively charged TrOCs used for their studies. In our previous study [22], both the CTA-NW and CTA-ES membranes were found to have a lower rejection of negatively charged PhACs especially of low molecular weights (Fig. 3). Madsen et al. [42] also pointed out that the CTA membranes did not perform well in rejecting a few of small neutral organic compounds. As such, whether a TFC membrane or a CTA membrane has a better rejection performance depends on the number of all the positively charged, negatively charged and neutral TrOCs selected for the study.

3.3. Impact of reverse draw solute diffusion

Above results showed that the nature of molecular charge of a TrOC had a great impact on its rejection by the TFC-ES membrane. It could be due to the electrostatic effect. At neutral pH, the zeta potential of the TFC-ES membrane surface was determined to be –15 mV. (In comparison, the CTA-ES and CTA-NW membranes carried much less surface charge with zeta potentials measured to be –4.5 and –6.5 mV at neutral pH, respectively.) The electrostatic interactions between charged solutes and membranes were extensively investigated in previous studies [43–45]. It was verified that for negatively charged membranes, electrostatic repulsion leads to an increase of the rejection of negatively charged solutes while electrostatic attraction leads to a decrease of the rejection of positively charged solutes, compared to neutral solutes.

The characteristic reverse draw solute diffusion of FO operation could also impact the rejection of charged species and lead to the difference in rejection between negatively and positively charged PhACs. To investigate this mechanism, the TFC-ES membrane was also operated in the RO mode to test its rejection of the same 21 PhACs. (The rejection was shown in Section 4 in the Supplemental File.) Eq. (3) was used to fit the rejection data and obtain the PhAC permeability coefficient in the RO mode ($B_{PhAC-RO}$). Note that Eq. (3) is applicable for both forward osmosis and reverse osmosis operations. The equation was also used to fit the FO rejection data and obtain the PhAC permeability coefficient in the FO mode ($B_{PhAC-FO}$). These two pairs of coefficients were compared for the difference. This method had also been used in our previous study [22].

It is clear that the $B_{PhAC-FO}$ values for all the eight positively charged PhACs were substantially larger than the $B_{PhAC-RO}$ values (Fig. 5). The main differences of the FO mode from the RO mode are the presence of reverse draw solute diffusion and the absence of hydraulic pressure. A previous study [46] showed that the active layer of TFC membranes was relatively compressible and as such would be denser and have a higher rejection when operated in the RO mode. However, this phenomenon was

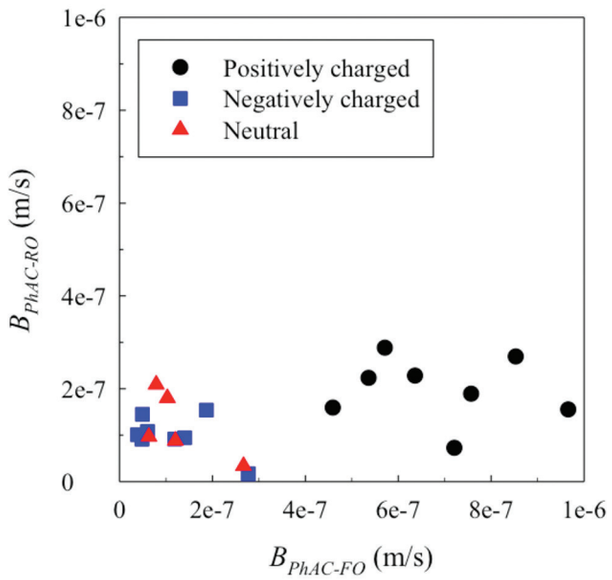

Fig. 5. Comparison of the $B_{PhAC-FO}$ and $B_{PhAC-RO}$ values for the TFC-ES membrane. The $B_{PhAC-FO}$ values were obtained from fitting the FO rejection ratios, while the $B_{PhAC-RO}$ values were obtained from fitting the rejection data in the RO mode, both by using Eq. (3).

not observed for the uncharged and negatively charged PhACs. (Note that, due to the reasonably small B_{PhAC} values for uncharged and negatively charged PhACs, uncontroversial comparison of the values obtained in the FO and RO modes was difficult to make. Nevertheless, the $B_{PhAC-FO}$ and $B_{PhAC-RO}$ values could be similar in that the data were scattered.) The difference was therefore unlikely due to the compression mechanism. Thus, it is reasonable to attribute the larger permeability coefficients in the FO mode for positively charged PhACs to the reverse draw solute diffusion.

Mutual interaction between the draw solution ions (e.g., NH_4^+) and the feed water ions (e.g., Na^+) was observed previously when TFC membrane was used, which substantially accelerated the loss of draw solute into the feed water [47]. The mechanism was speculated to be "ion exchange". The results described above showed that mutual interaction also exists between inorganic ions in draw solution and ionic organics in feed water. The underlying mechanism could also be "ion exchange" with positively charged ions involved. Due to the higher concentration of Na^+ ions in the draw solution side and the electrostatic attraction to the negatively charged membrane surface, they would spontaneously diffuse through the membrane from the DS to the FW (i.e., reverse diffusion). To maintain the solution electroneutrality, either reverse diffusion of counterions (i.e., Cl^-) or forward transport of positively charged PhACs was needed. The negative charge of the membrane would hinder the reverse transport of counterions to some extent thus facilitating the diffusion of the positively charged PhACs. This mechanism made additional contribution to the transport rate of positively charged PhACs and resulted in lower rejections than expected. In our previous study [22] in which CTA membranes were used, the reverse draw solute (NaCl) diffusion was found to impair the rejection of some negatively charged PhACs. In comparison to the TFC-ES membrane, the CTA membranes were only weakly negatively charged. The difference in surface charge density might be responsible for the difference in PhACs which were substantially affected by the reverse draw solute diffusion. Nevertheless, the physicochemical principles governing the "ion exchange" inside the membrane during FO operation remains yet to be known and requires further investigation.

3.4. Roles of steric and hydrophobic effects

Size exclusion is a critical mechanism for dense membranes in rejecting the contaminants from water [16,48]. It was described above that, for the negatively charged PhACs, a larger molecular weight generally corresponded to a higher rejection (Fig. 3). To further investigate the role of steric effect in affecting the rejection by the TFC-ES membrane, the B_{PhAC} value (obtained in FO mode) for each selected PhAC was plotted as a function of the molecular weight (Fig. 6). It was shown that for all the selected PhACs, the relation of the B_{PhAC} values to the molecular weight was not noticeable. For most of the selected PhACs, the molecular weight has a good linear relation with the Stokes radius (Section 5 in the Supplemental File). Thus, similar results could be obtained when relating the B_{PhAC} values to the Stokes radius. It indicated that steric exclusion was not the predominant rejection mechanism here especially for the positively charged PhACs. It might not be appropriate to estimate the MWCO of the TFC-ES membrane from the B_{PhAC} values of the limited number of uncharged and negatively charged PhACs. Nevertheless, if a MWCO comparable to that for the CTA-ES and CTA-NW membranes (approximately within 250–350 Da [22]) was assumed for the TFC-ES membrane, the effect of steric effect on the B_{PhAC} values (and the rejections) of both uncharged and negatively charged PhACs was reasonable.

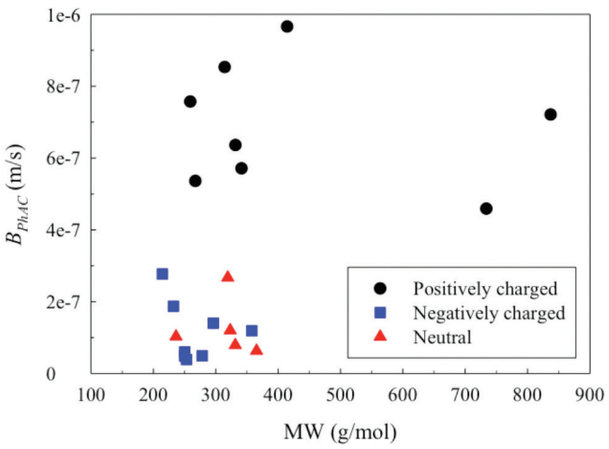

Fig. 6. Dependence of the B_{PhAC} values (obtained in the FO mode) on the molecular weight for the selected PhACs when the TFC-ES membrane was used.

The rejections of glucose (in the RO mode) were compared to indicate the relative "pore" sizes of the three membranes. Glucose is a hydrophilic neutral organic compound which was expected to have little electrostatic or hydrophobic interaction with the membrane. Based on the results (Fig. 7), it appears that the TFC-ES membrane might have a larger MWCO (or pore size) than the less compact CTA-ES membrane, and the more compact CTA-NW membrane too. It revealed that, compared with that for the two CTA membranes, steric effect might play a somewhat less significant role in rejecting PhACs by the TFC-ES membrane. It might partly explain the slightly poorer performance in rejecting most neutral PhACs (Fig. 3).

In addition to the steric and electrostatic effects, the difference of the three membranes in rejecting PhACs would also be partly because of the PhAC-membrane interactions. Previous studies indicated that the solutes with a higher affinity for the membrane material could partition into the membrane matrix more easily and subsequently diffuse through the membrane at a higher rate, leading to a lower rejection [49,50]. The solute–membrane affinity could be primarily due to hydrophobic effect, and could also include some specific interactions such as hydrogen bonding and π–π stacking [29,51]. (π–π stacking is a possible supramolecular interaction between membrane polymers and organic solutes when the membrane polymer has electron deficient aromatic groups and the organic compound contains aromatic π-systems or functional groups with free electron pairs.) Though the log P or log D value of an organic compound was widely used as a parameter to indicate its hydrophobicity, it might be more appropriate to quantify the hydrophobic effect between the solute and membrane by using their interaction free energy (ΔG_i). A more negative value of ΔG_i indicates a stronger solute–membrane affinity and an easier partitioning of solute into membrane matrix. Zhang et al. [52] demonstrated that incorporating ΔG_i into the steric model could dramatically improve the model prediction accuracy of rejection by TFC NF and RO membranes. The surface free energy components of each membranes could be obtained from the surface free energy components of three liquids and the measurement results of contact angles for the three membranes. (More details were shown in Section 6 in the Supplemental File.) The surface free energy components of a few PhACs were also listed [30,53]. As such, the ΔG_i values for the interactions of these PhACs with each membrane could be calculated (Table 3). Results showed that almost all the ΔG_i values were negative, indicating that these PhACs might have a certain affinity to the membranes resulted from the hydrophobic effects, which could have some impact on the transport and rejection of PhACs. For carbamazepine, the most negative ΔG_i value for the CTA-ES membrane might partly explain its lower rejection than the other two membranes.

The quantification of specific interactions could be much more difficult. However, the impact of specific interactions on rejection is fairly evident. For example, Chappell et al. [54] demonstrated that the hydrogen bonds between the N-alkyl group of atrazine and acetylated hydroxyl groups of CTA membranes might facilitate the transport of atrazine by swelling its concentration in membrane polymer. It was pointed out that the TFC membranes mainly comprising of aromatic polyamides could probably have a high capacity to form hydrogen bonding or π–π interaction with organic solutes [55]. More attentions should be paid to understanding and, if possible, quantification of these specific interactions.

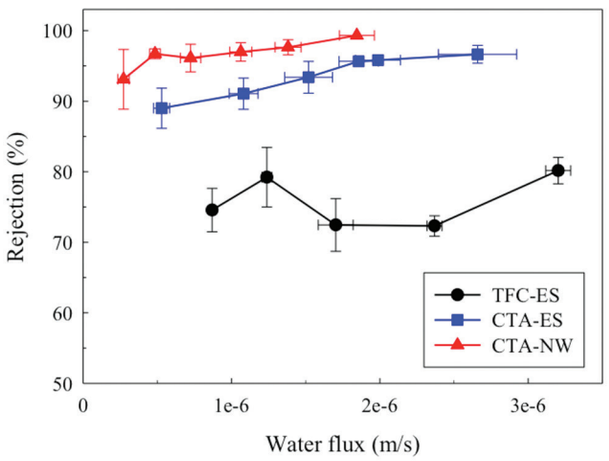

Fig. 7. Rejection of glucose by the three membranes as a function of water flux.

4. Conclusions

The performance of the TFC-ES FO membrane in rejecting a total of 21 PhACs was tested and compared to that of the CTA-ES and CTA-NW membranes reported previously. Results showed that the TFC-ES membrane had a higher water permeability and salt rejection ability, but a generally lower rejection of the PhACs than both CTA membranes. When the draw solute concentration was sufficiently high (e.g., 2 M), all PhACs could be well rejected by the TFC-ES membrane with a rejection higher than 85%, but the rejection of positively charged PhACs was substantially lower than that of negatively charged and neutral PhACs. The low rejection of positively charged PhACs by the TFC-ES membrane was partly due to the negative surface charge of the membrane, and partly caused by the reverse draw solute diffusion. The "ion exchange" mechanism might be responsible for the effect of reverse draw solute diffusion. In addition

Table 3
Interaction free energies between PhACs and membranes

Pharmaceutical	ΔG_i (10^{-21} J)		
	TFC-ES	CTA-ES	CTA-NW
Metoprolol	–10.59	–15.23	–9.71
Propranolol	–1.02	–5.48	–0.08
Carbamazepine	–3.43	–6.73	–2.77
Gemfibrozil	–17.27	–22.13	–16.40
Clofibric acid	–2.48	–5.56	–1.84
Diclofenac	–0.17	–4.15	0.79
Sulfamethoxazole	–9.53	–12.88	–9.02

to steric exclusion and electrostatic interaction, hydrophobic effects could also play an important role in rejection of some PhACs, such as carbamazepine. The effect of specific solute–membrane interactions on the transport of organic solutes and rejection by the FO membranes should also be taken into consideration in future study. Though the TFC-ES membrane provided by HTI is no longer commercialized, the performance and rejection mechanisms revealed here are representative and can provide reference for the investigation of other TFC FO membranes. The results indicate that, for a better exploitation of the TFC FO membranes, the performance in rejecting TrOCs needs to be further improved.

Acknowledgments

The authors acknowledge the financial support provided by the National Natural Science Foundation of China (No. 51278268) and the Beijing Municipal Natural Science Foundation (No. 8132043).

References

[1] T.Y. Cath, A.E. Childress, M. Elimelech, Forward osmosis: Principles, applications, and recent developments, J. Membr. Sci., 281 (2006) 70–87.
[2] G. Blandin, A.R.D. Verliefde, C.Y. Tang, P. Le–Clech, Opportunities to reach economic sustainability in forward osmosis–reverse osmosis hybrids for seawater desalination, Desalination, 363 (2015) 26–36.
[3] R.L. McGinnis, M. Elimelech, Energy requirements of ammonia–carbon dioxide forward osmosis desalination, Desalination, 207 (2007) 370–382.
[4] J.R. McCutcheon, R.L. McGinnis, M. Elimelech, A novel ammonia—carbon dioxide forward (direct) osmosis desalination process, Desalination, 174 (2005) 1–11.
[5] J. Webley, Technology developments in forward osmosis to address water purification, Desal. Water Treat., 55 (2015) 2612–2617.
[6] T.-S. Chung, S. Zhang, K.Y. Wang, J. Su, M.M. Ling, Forward osmosis processes: Yesterday, today and tomorrow, Desalination, 287 (2012) 78–81.
[7] R.V. Linares, Z.Y. Li, S. Sarp, Y.G. Park, G. Amy, J.S. Vrouwenvelder, Higher boron rejection with a new TFC forward osmosis membrane, Desal. Water Treat., 55 (2015) 2734–2740.
[8] W. Fam, S. Phuntsho, J.H. Lee, H.K. Shon, Performance comparison of thin-film composite forward osmosis membranes, Desal. Water Treat., 51 (2013) 6274–6280.
[9] R.P. Schwarzenbach, B.I. Escher, K. Fenner, T.B. Hofstetter, C.A. Johnson, U. von Gunten, B. Wehrli, The challenge of micropollutants in aquatic systems, Science, 313 (2006) 1072–1077.
[10] B.D. Coday, B.G.M. Yaffe, P. Xu, T.Y. Cath, Rejection of trace organic compounds by forward osmosis membranes: A literature review, Environ. Sci. Technol., 48 (2014) 3612–3624.
[11] R.M. Abousnina, L.D. Nghiem, Removal of dissolved organics from produced water by forward osmosis, Desal. Water Treat., 52 (2014) 570–579.
[12] R. Valladares Linares, V. Yangali-Quintanilla, Z. Li, G. Amy, Rejection of micropollutants by clean and fouled forward osmosis membrane, Water Res., 45 (2011) 6737–6744.
[13] N.T. Hancock, P. Xu, D.M. Heil, C. Bellona, T.Y. Cath, Comprehensive bench- and pilot-scale investigation of trace organic compounds rejection by forward osmosis, Environ. Sci. Technol., 45 (2011) 8483–8490.
[14] M. Xie, L.D. Nghiem, W.E. Price, M. Elimelech, Relating rejection of trace organic contaminants to membrane properties in forward osmosis: Measurements, modelling and implications, Water Res., 49 (2014) 265–274.
[15] J. Ren, J.R. McCutcheon, A new commercial thin film composite membrane for forward osmosis, Desalination, 343 (2014) 187–193.
[16] C. Bellona, J.E. Drewes, P. Xu, G. Amy, Factors affecting the rejection of organic solutes during NF/RO treatment–a literature review, Water Res., 38 (2004) 2795–2809.
[17] X.-M. Wang, B. Li, T. Zhang, X.-Y. Li, Performance of nanofiltration membrane in rejecting trace organic compounds: Experiment and model prediction, Desalination, 370 (2015) 7–16.
[18] H.Y. Yang, X.M. Wang, Mechanism of removal of pharmaceuticals and personal care products by nanofiltration membranes, Desal. Water Treat., 53 (2015) 2816–2824.
[19] X. Jin, J. Shan, C. Wang, J. Wei, C.Y. Tang, Rejection of pharmaceuticals by forward osmosis membranes, J. Hazard. Mater., 227 (2012) 55–61.
[20] Y. Zheng, M. Huang, L. Chen, W. Zheng, P. Xie, Q. Xu, Comparison of tetracycline rejection in reclaimed water by three kinds of forward osmosis membranes, Desalination, 359 (2015) 113–122.
[21] M. Xie, L.D. Nghiem, W.E. Price, M. Elimelech, Comparison of the removal of hydrophobic trace organic contaminants by forward osmosis and reverse osmosis, Water Res., 46 (2012) 2683–2692.
[22] F.-X. Kong, H.-W. Yang, Y.-Q. Wu, X.-M. Wang, Y.F. Xie, Rejection of pharmaceuticals during forward osmosis and prediction by using the solution–diffusion model, J. Membr. Sci., 476 (2015) 410–420.
[23] J.G. Wijmans, R.W. Baker, The solution-diffusion model: A review, J. Membr. Sci., 107 (1995) 1–21.
[24] C.Y. Tang, Q. She, W.C.L. Lay, R. Wang, A.G. Fane, Coupled effects of internal concentration polarization and fouling on flux behavior of forward osmosis membranes during humic acid filtration, J. Membr. Sci., 354 (2010) 123–133.
[25] C. Suh, S. Lee, Modeling reverse draw solute flux in forward osmosis with external concentration polarization in both sides of the draw and feed solution, J. Membr. Sci., 427 (2013) 365–374.
[26] N.-N. Bui, J.T. Arena, J.R. McCutcheon, Proper accounting of mass transfer resistances in forward osmosis: Improving the accuracy of model predictions of structural parameter, J. Membr. Sci., 492 (2015) 289–302.
[27] C.J.V. Oss, Interfacial Forces in Aqueous Media, 2nd ed., Taylor & Francis, Boca Raton, USA, 2006.
[28] C.J.V. Oss, M.K. Chaudhury, R.J. Good, Interfacial Lifshitz-van der Waals and polar interactions in macroscopic systems, Chem. Rev., 88 (1988) 927–941.
[29] A.R.D. Verliefde, E.R. Cornelissen, S.G.J. Heijman, E.M.V. Hoek, G.L. Amy, B. Van Der Bruggen, J.C. Van Dijk, Influence of solute-membrane affinity on rejection of uncharged organic solutes by nanofiltration membranes, Environ. Sci. Technol., 43 (2009) 2400–2406.
[30] S. Botton, A.R.D. Verliefde, N.T. Quach, E.R. Cornelissen, Influence of biofouling on pharmaceuticals rejection in NF membrane filtration, Water Res., 46 (2012) 5848–5860.
[31] T. Masuko, A. Minami, N. Iwasaki, T. Majima, S.I. Nishimura, C.L. Yuan, Carbohydrate analysis by a phenol–sulfuric acid method in microplate format, Anal. Biochem., 339 (2005) 69–72.
[32] K. Gerstandt, K.V. Peinemann, S.E. Skilhagen, T. Thorsen, T. Holt, Membrane processes in energy supply for an osmotic power plant, Desalination, 224 (2008) 64–70.
[33] A. Tiraferri, N.Y. Yip, W.A. Phillip, J.D. Schiffman, M. Elimelech, Relating performance of thin-film composite forward osmosis membranes to support layer formation and structure, J. Membr. Sci., 367 (2011) 340–352.
[34] N.Y. Yip, A. Tiraferri, W.A. Phillip, J.D. Schiffman, M. Elimelech, High performance thin-film composite forward osmosis membrane, Environ. Sci. Technol., 44 (2010) 3812–3818.
[35] B.D. Coday, C. Hoppe-Jones, D. Wandera, J. Shethji, J. Herron, K. Lampi, S.A. Snyder, T.Y. Cath, Evaluation of the transport parameters and physiochemical properties of forward osmosis membranes after treatment of produced water, J. Membr. Sci., 499 (2016) 491–502.

[36] T.Y. Cath, M. Elimelech, J.R. McCutcheon, R.L. McGinnis, A. Achilli, D. Anastasio, A.R. Brady, A.E. Childress, I.V. Farr, N.T. Hancock, J. Lampi, L.D. Nghiem, M. Xie, N.Y. Yip, Standard methodology for evaluating membrane performance in osmotically driven membrane processes, Desalination, 312 (2013) 31–38.
[37] T.P.N. Nguyen, B.M. Jun, J.H. Lee, Y.N. Kwon, Comparison of integrally asymmetric and thin film composite structures for a desirable fashion of forward osmosis membranes, J. Membr. Sci. 495 (2015) 457–470.
[38] G. Blandin, A.R.D. Verliefde, C.Y. Tang, A.E. Childress, P. Le-Clech, Validation of assisted forward osmosis (AFO) process: Impact of hydraulic pressure, J. Membr. Sci., 447 (2013) 1–11.
[39] A. Tiraferri, N.Y. Yip, A.P. Straub, S. Romero-Vargas Castrillon, M. Elimelech, A method for the simultaneous determination of transport and structural parameters of forward osmosis membranes, J. Membr. Sci., 444 (2013) 523–538.
[40] M. Huang, Y. Chen, C.-H. Huang, P. Sun, J. Crittenden, Rejection and adsorption of trace pharmaceuticals by coating a forward osmosis membrane with TiO_2, Chem. Eng. J., 279 (2015) 904–911.
[41] G. Blandin, H. Vervoort, A. D'Haese, K. Schoutteten, J.V. Bussche, L. Vanhaecke, D.T. Myat, P. Le-Clech, A.R.D. Verliefde, Impact of hydraulic pressure on membrane deformation and trace organic contaminants rejection in pressure assisted osmosis (PAO), Process Safety Environ. Protect., 102 (2016) 316–327.
[42] H.T. Madsen, N. Bajraktari, C. Hélix-Nielsen, B. Van der Bruggen, E.G. Søgaard, Use of biomimetic forward osmosis membrane for trace organics removal, J. Membr. Sci., 476 (2015) 469–474.
[43] M. Vanoppen, A.F.A.M. Bakelants, D. Gaublomme, K.V.K.M. Schoutteten, J.V. Bussche, L. Vanhaecke, A.R.D. Verliefde, Properties governing the transport of trace organic contaminants through ion-exchange membranes, Environ. Sci. Technol., 49 (2015) 489–497.
[44] A.R.D. Verliefde, E.R. Cornelissen, S.G.J. Heijman, J.Q.J.C. Verberk, G.L. Amy, B.V.D. Bruggen, J.C.V. Dijk, The role of electrostatic interactions on the rejection of organic solutes in aqueous solutions with nanofiltration, J. Membr. Sci., 322 (2008) 52–66.
[45] L.D. Nghiem, A.I. Schäfer, M. Elimelech, Role of electrostatic interactions in the retention of pharmaceutically active contaminants by a loose nanofiltration membrane, J. Membr. Sci., 286 (2006) 52–59.
[46] B.D. Coday, D.M. Heil, P. Xu, T.Y. Cath, Effects of transmembrane hydraulic pressure on performance of forward osmosis membranes, Environ. Sci. Technol., 47 (2013) 2386–2393.
[47] X. Lu, C. Boo, J. Ma, M. Elimelech, Bidirectional diffusion of ammonium and sodium cations in forward osmosis: Role of membrane active layer surface chemistry and charge, Environ. Sci. Technol., 48 (2014) 14369–14376.
[48] H.Q. Dang, L.D. Nghiem, W.E. Price, Factors governing the rejection of trace organic contaminants by nanofiltration and reverse osmosis membranes, Desal. Water Treat., 52 (2014) 589–599.
[49] K. Kimura, G. Amy, J. Drewes, Y. Watanabe, Adsorption of hydrophobic compounds onto NF/RO membranes: an artifact leading to overestimation of rejection, J. Membr. Sci., 221 (2003) 89–101.
[50] J.M. Arsuaga, M.J. López-Muñoz, A. Sotto, G. Del Rosario, Retention of phenols and carboxylic acids by nanofiltration/reverse osmosis membranes: Sieving and membrane-solute interaction effects, Desalination, 200 (2006) 731–733.
[51] A.I. Schäfer, I. Akanyeti, A.J.C. Semião, Micropollutant sorption to membrane polymers: A review of mechanisms for estrogens, Adv. Colloid Interface Sci., 164 (2011) 100–117.
[52] Y. Zhang, G. Maes, B. Bruggen, C. Vandecasteele, Influence of hydrophobicity on retention in nanofiltration of aqueous solutions containing organic compounds, J. Membr. Sci., 252 (2005) 195–203.
[53] D.J.D. Ridder, A.R.D. Verliefde, K. Schoutteten, B.V.D. Linden, S.G.J. Heijman, I. Beurroies, R. Denoyel, G.L. Amy, J.C.V. Dijk, Relation between interfacial energy and adsorption of organic micropollutants onto activated carbon, Carbon, 53 (2013) 153–160.
[54] M.A. Chappell, D.A. Laird, M.L. Thompson, H. Li, B.J. Teppen, V. Aggarwal, C.T. Johnston, S.A. Boyd, Influence of smectite hydration and swelling on atrazine sorption behavior, Environ. Sci. Technol., 39 (2005) 3150–3156.
[55] J. Heo, L.K. Boateng, J.R.V. Flora, H. Lee, N. Her, Y.G. Park, Y. Yoon, Comparison of flux behavior and synthetic organic compound removal by forward osmosis and reverse osmosis membranes, J. Membr. Sci., 443 (2013) 69–82.

S1. Calculation of the mass transfer coefficient (*k*)

The mass transfer coefficient *k* can be calculated through the Sherwood number for the appropriate flow regime in a rectangular channel.

$$Sh = 1.85\left(\mathrm{Re}\,Sc\frac{d_h}{L}\right)^{0.33} \tag{S1}$$

Here, Re is the Reynolds number, *Sc* is the Schmidt number, d_h is the hydraulic diameter, and *L* is the length of channel. The mas transfer coefficient, *k*, is related to *Sh* by

$$k = \frac{ShD}{d_h} \tag{S2}$$

where *D* is the solute diffusion coefficient.

S2. Calculation of the PhAC-membrane interaction free energy (ΔG_i)

The PhAC-membrane interaction free energy (ΔG_i) was calculated from the surface free energy components of the PhAC and the membrane by

$$\Delta G_i = 2A_s\left[\begin{array}{l}\sqrt{\gamma_s^{LW}\gamma_w^{LW}}+\sqrt{\gamma_m^{LW}\gamma_w^{LW}}-\sqrt{\gamma_m^{LW}\gamma_s^{LW}}-\gamma_w^{LW}+\sqrt{\gamma_w^{+}}\left(\sqrt{\gamma_s^{-}}+\sqrt{\gamma_m^{-}}-\sqrt{\gamma_w^{-}}\right)\\ +\sqrt{\gamma_w^{-}}\left(\sqrt{\gamma_s^{+}}+\sqrt{\gamma_m^{+}}-\sqrt{\gamma_w^{+}}\right)-\sqrt{\gamma_m^{-}\gamma_s^{+}}-\sqrt{\gamma_m^{+}\gamma_s^{-}}\end{array}\right] \tag{S3}$$

where γ^{LW} is the Lifshitz–van der Waals component, γ^+ is the Lewis Acid–Base electron acceptor component and γ^- is the Lewis Acid–Base electron donor component. The subscripts, *s*, *w* and *m* refer to PhAC, water and membrane, respectively. A_s is the contact area of the PhAC with the membrane which could be calculated from the PhAC Stokes radius (r_s) by $A_s = r_s^2/2$.

The surface free energy components of the FO membranes were determined by measuring contact angles using three different liquids (i.e., water, diiodomethane and formamide) on the membrane surface and solving the Young-Dupré equation

$$(1+\cos\theta)\gamma_L = 2(\sqrt{\gamma_s^{LW}\gamma_L^{LW}}+\sqrt{\gamma_s^{+}\gamma_L^{-}}+\sqrt{\gamma_s^{-}\gamma_L^{+}}) \tag{S4}$$

Here, the subscript L refers to the liquid and θ is the contact angle of the membrane using this kind of liquid. γ_L is the surface tension of liquids which could be obtained by $\gamma_L = \gamma_L^{LW} + 2\sqrt{\gamma_L^{+}\gamma_L^{-}}$. The surface free energy components of the three liquids and certain PhACs were available in the literature.

S3. Reverse draw solute flux as a function of water flux.

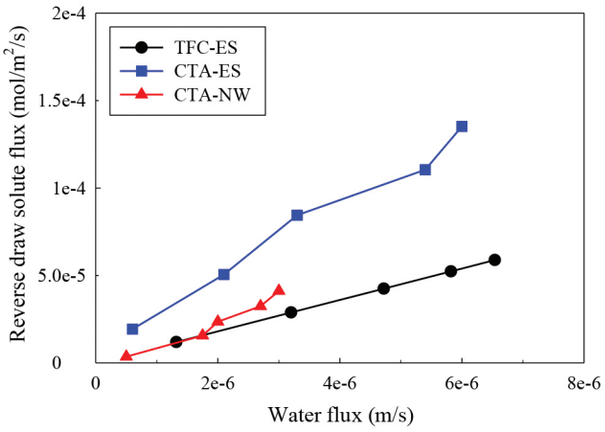

Fig. S1. The reverse draw solute fluxes of the three membranes as a function of water flux.

S4. Rejection of PhACs by the TFC-ES membrane in the RO mode.

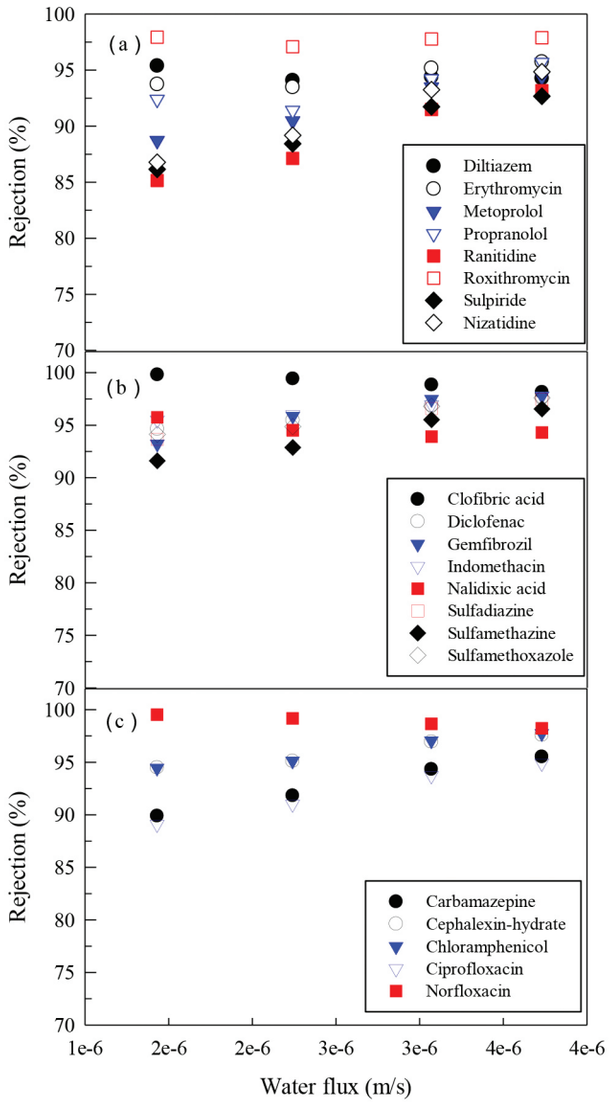

Fig. S2. Rejections of (a) positively charged PhACs (b) negatively charged PhACs and (c) neutral PhACs by the TFC-ES membrane in the RO mode.

S5. Correlation between molecular weight and Stokes radius for the selected PhACs.

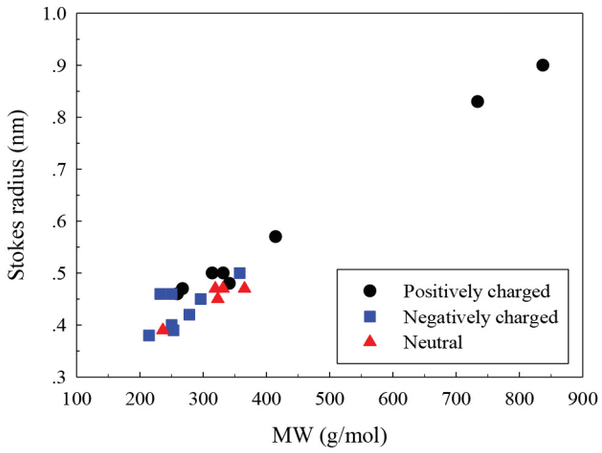

Fig. S3. Correlation between the molecular weight and the Stokes radius for the selected PhACs.

S6. Calculation of the surface free energy components of membranes.

Table S1
Contact angles of membranes and surface free energy parameters of three liquids

Liquid	θ of TFC-ES	θ of CTA-ES	θ of CTA-NW	γ_L^{LWa} (mJ/m²)	γ_L^{+a} (mJ/m²)	γ_L^{-a} (mJ/m²)
Water	75.6	80.7	72.1	21.8	25.5	25.5
Diiodomethane	50.2	32.6	47.2	50.8	0	0
Formamide	54.6	50.3	51.8	39.0	2.28	39.6

[a] data from Ref. [33].

Table S2
Surface free energy parameters of solutes and membranes.

Membrane or solute	γ^{LW} (mJ/m²)	γ^+ (mJ/m²)	γ^- (mJ/m²)
TFC-ES	34.2	0.65	7.8
CTA-ES	43.1	0.4	2.8
CTA-NW	35.8	0.6	9.7
Water[a]	21.8	25.5	25.5
Metoprolol[a]	41.9	0.1	20.0
Propranolol[a]	47.0	0.0	63.7
Carbamazepine[a]	46.5	0.0	44.1
Gemfibrozil[a]	39.1	0.0	4.2
Clofibric acid[a]	45.4	0.0	49.3
Diclofenac[a]	39.3	0.0	65.9
Sulfamethoxazole[b]	49.1	0.3	11.5

[a] data from Ref. [30]; [b] data from Ref. [53].